The Effect of Waste Loading and Glass Structural Factors on Structure and Chemical Durability of SB2 and SB4 SRS Waste Glasses - 11397

S.V. Stefanovsky,
SIA RADON, 7th Rostovskii lane 2/14, Moscow 119121 Russia, profstef@mtu-net.ru

J.C. Marra
Savannah River National Laboratory, Building 773-A, Aiken, SC 29808 USA

ABSTRACT

Glassy materials simulating vitrified high-Na/Fe (Sludge Batch 2 – SB2) and high-Na/Fe/Al (Sludge Batch 4 – SB4) Savannah River Site high level wastes (HLW) were produced in a resistive furnace and 236 and 418 mm inner diameter cold crucibles. The effect of waste loading (WL) and glass structural factors (degree of connectedness of glass network, metal oxides to boron oxide ratios) on chemical durability of glassy materials was studied.

INTRODUCTION

Results of collaborative work between Savannah River National Laboratory (SRNL, USA) and SIA Radon (Russia) demonstrated feasibility of vitrification of high-Na/Fe (SB2) and high-Na/Fe/Al (SB4) wastes using a cold crucible induction melter (CCIM) were described in numerous papers (see, for example, [1-4]. The materials produced were composed of major vitreous and minor spinel structure phase at WLs of 40 to 55 wt.% and extra nepheline phase at WLs of ~60 wt.% and higher. Total content of crystalline constituent increased with WL. Leaching measurements also showed increasing of normalized release rates of B, Li, Na and Si with the increase of waste loading. In the present paper, the effect of various structural factors (degree of connectedness of glass network, metal oxides to boron oxide ratios) on the structure and chemical durability of the glassy products was analyzed.

EXPERIMENTAL

Glassy materials simulating vitrified SB2 and SB4 HLW (Table I and II) were produced in a resistive furnace at temperatures of up to 1400 °C and 236 and 418 mm inner diameter cold crucibles energized from 60 kW/1.76 MHz and 160 kW/1.76 MHz generators at Radon bench- and full-scale plants, respectively, described in our previous works [1-4].

The materials produced were examined with infrared (IR) spectroscopy using a modernized IKS-29 spectrophotometer (compaction of powdered glass in pellets with KBr). Chemical durability of the materials was determined by the Product Consistency Test – Method A (PCT-A) [5].

THEORETICAL REMARKS

Various structural factors were suggested to describing the structure of glasses. The most general factor is a degree of connectedness determined as

Table I. Chemical compositions (wt.%) of waste surrogates, frits and SRS waste glasses.

Oxides	SB2					SB4				
	SB2 HLW surrogate	Frit 320	Glass (40% WL)	Glass (50% WL)	Glass (60% WL)	SB4 HLW surrogate	Frit 503-R4	Glass (40% WL)	Glass (50% WL)	Glass (60% WL)
Li_2O	-	8.00	4.80	4.00	3.20	-	8.00	4.80	4.00	3.20
B_2O_3	-	8.00	4.80	4.00	3.20	-	16.00	9.60	8.00	6.40
F	0.01	-	-	0.005	0.01	-	-	-	-	-
Na_2O	12.08	12.00	12.03	12.04	12.05	18.71	-	7.48	9.35	11.22
MgO	0.24	-	0.10	0.12	0.14	2.77	-	1.11	1.39	1.66
Al_2O_3	16.83	-	6.73	8.415	10.10	25.49	-	10.20	12.75	15.29
SiO_2	1.98	72.00	43.99	36.99	30.00	2.71	76.00	46.68	39.36	32.03
P_2O_5	0.14	-	0.06	0.07	0.08	-	-	-	-	-
SO_3	0.83	-	0.33	0.41	0.50	0.87	-	0.35	0.43	0.52
Cl	1.51	-	0.60	0.75	0.90	-	-	-	-	-
K_2O	0.09	-	0.04	0.045	0.05	0.07	-	0.03	0.03	0.04
CaO	3.76	-	1.50	1.88	2.25	2.77	-	1.11	1.38	1.66
TiO_2	-	-	-	-	-	0.04	-	0.02	0.02	0.02
Cr_2O_3	0.37	-	0.15	0.185	0.22	0.20	-	0.01	0.10	0.12
MnO	3.89	-	1.56	1.945	2.33	5.78	-	2.31	2.89	3.47
Fe_2O_3	42.24	-	16.90	21.12	25.36	28.99	-	11.60	14.49	17.39
NiO	2.17	-	0.87	1.085	1.30	1.66	-	0.67	0.83	1.00
CuO	0.20	-	0.08	0.10	0.12	0.05	-	0.02	0.03	0.03
ZnO	0.39	-	0.16	0.195	0.23	0.05	-	0.02	0.02	0.03
SrO	0.10	-	0.04	0.05	0.06	-	-	-	-	-
ZrO_2	0.79	-	0.32	0.395	0.47	0.09	-	0.04	0.05	0.05
I	0.04	-	0.02	0.02	0.03	-	-	-	-	-
BaO	0.27	-	0.11	0.135	0.16	0.07	-	0.03	0.03	0.04
PbO	0.32	-	0.13	0.16	0.19	0.38	-	0.15	0.19	0.23
U_3O_8	11.75	-	4.70	5.875	7.05	9.03	-	3.61	4.52	5.42
Ce_2O_3	-	-	-	-	-	0.21	-	0.08	0.11	0.13
La_2O_3	-	-	-	-	-	0.03	-	0.1	0.02	0.02
ThO_2[b]	-	-	-	-	-	0.02	-	0.01	0.02	0.02
Total	100	100	100	100	100	100	100	100	100	100

$$f_{Si} = [Si]/[O] = [SiO_2]/([Me_2O]+[MeO]+3[Me_2O_3]+2[MeO_2]+5[Me_2O_5]+3[MeO_3]) \quad (1),$$

where atomic and molar fractions of the elements or oxides, respectively, are given in square brackets. The value of $f_{Si} = 0.33$ is considered to be a limit for glass formation. Glasses at $f_{Si} < 0.33$ should not form. However, there are so-called inverted glasses that do not satisfy this condition.

In the glasses of the Me_2O-Al_2O_3-SiO_2 system as well as crystalline aluminosilicates, aluminum may be present in both tetrahedral and octahedral oxygen environment. At $[Me_2O]/[Al_2O_3]>1$ Al^{3+} ions are tetrahedrally coordinated and form $[(AlO_{4/2})^-Na^+]$ network-forming units. In alkali free and low-alkali glasses especially containing small radii alkali earth cations (Be^{2+}, Mg^{2+}), Al^{3+} ions are six-coordinated and play a role as network-modifiers.

Table II. Molar concentrations of major constituents in actual glasses with target WLs and vitreous phases of the glassy materials recalculated to 100%.

Oxides	WL in SB2 waste glasses, wt.%											
	40	45		50		55		60		65		70
	bulk	bulk	vf	bulk	vf	bulk	vf	bulk	vf	bulk	vf	bulk
Al_2O_3	4.84	5.66	5.55	6.56	5.96	7.52	7.01	8.56	8.10	9.71	10.11	10.97
B_2O_3	5.03	4.80	4.80	4.54	4.56	4.26	4.24	3.95	3.87	3.62	3.42	3.26
CaO	1.97	2.30	2.26	2.67	2.68	3.06	3.18	3.49	4.21	3.95	4.59	4.46
Fe_2O_3	7.76	9.07	8.07	10.49	9.10	12.03	10.32	13.71	8.09	15.55	6.73	17.56
Li_2O	11.75	11.19	11.19	10.59	10.64	9.94	9.89	9.23	9.04	8.45	7.98	7.60
Na_2O	14.25	14.82	14.60	15.42	15.44	16.08	15.32	16.81	18.60	17.60	19.45	18.47
SiO_2	53.83	51.49	52.87	48.96	50.85	46.22	49.16	43.23	47.07	39.98	46.50	36.39
U_3O_8	0.57	0.67	0.66	0.77	0.78	0.89	0.89	1.01	1.03	1.15	1.22	1.29
Total	100.00	100.00	100.00	100.00	100.00	100.00	100.00	100.00	100.00	100.00	100.00	100.00
f_{Si}	0.28	0.27	0.28	0.25	0.27	0.24	0.25	0.22	0.25	0.20	0.25	0.18
ψ_B	2.84	2.94	2.92	3.07	3.19	3.21	3.19	3.40	4.17	3.64	4.37	3.96
ψ_B (Fe)	2.38	2.38	2.41	2.37	2.59	2.37	2.46	2.36	3.54	2.35	3.78	2.35
	WL in SB4 waste glasses, wt.%											
	40	45	50		55		60		65		70 (66)	66
	bulk	bulk	bulk	vf	bulk	vf	bulk	vf	bulk	vf	bulk	vf
Al_2O_3	6.90	7.94	9.07	8.58	10.26	11.74	11.53	14.37	12.87	17.28	14.29	17.71
B_2O_3	9.47	8.88	8.30	8.23	7.68	7.10	7.03	6.38	6.34	5.77	5.60	5.03
CaO	1.37	1.56	1.79	1.57	2.03	3.12	2.28	3.61	2.55	4.30	2.83	4.35
Fe_2O_3	5.01	5.76	6.57	6.32	7.44	4.96	8.36	2.64	9.33	3.55	10.36	1.88
Li_2O	11.05	10.36	9.68	9.60	8.96	8.28	8.20	7.44	7.40	6.74	6.54	5.87
MgO	1.92	2.21	2.52	2.70	2.86	2.90	3.19	2.68	3.57	3.27	3.96	2.68
MnO	2.25	2.59	2.95	3.17	3.34	3.00	3.76	2.80	4.20	3.73	4.66	2.86
Na_2O	8.33	9.59	10.95	10.41	12.39	11.62	13.92	13.05	15.54	16.97	17.26	17.41
SiO_2	53.71	50.64	47.62	48.84	44.42	46.63	41.05	46.33	37.45	37.60	33.64	41.31
U_3O_8	0.41	0.47	0.54	0.58	0.61	0.65	0.69	0.71	0.77	0.79	0.85	0.89
Total	100.00	100.00	100.00	100.00	100.00	100.00	100.00	100.00	100.00	100.00	100.00	100.00
f_{Si}	0.27	0.25	0.24	0.25	0.22	0.24	0.20	0.24	0.19	0.19	0.17	0.21
ψ_B	0.67	0.75	0.83	0.92	0.94	0.89	1.08	0.80	1.25	1.18	1.48	1.23
ψ_B (Fe)	0.51	0.55	0.60	0.69	0.65	0.68	0.72	0.67	0.81	1.00	0.93	1.11

The structure of borosilicate glasses normally used for HLW immobilization is strongly dependent on the coordination state of boron and silica content. In vitreous B_2O_3 and binary borosilicate glasses, all the boron is ternary-coordinated forming boron-oxygen triangles linked in boroxole rings. Incorporation of minor alkali oxide (for example, Na_2O) at a ratio of ψ_B= =$[Na_2O]/[B_2O_3]$<1/3 keeps boron ternary-coordinated but the number of bridging oxygen ions decreases from 3 to 2. In this compositional range, two structural networks co-exist and thermal treatment results in metastable liquid-liquid phase separation with formation of high-silica and alkali-borate microareas. Further introduction of alkali oxides at ψ_B= $[Na_2O]/B_2O_3]$>1/3 leads to

formation of BO_4 tetrahedra yielding $[(BO_{4/2})^-Na^+]$ units. Formally all the boron should be completely transformed into tetrahedral coordinaton at $\psi_B = [Na_2O]:[B_2O_3]=1$ but actually some fraction of oxygen introduced with alkali oxides is spent for destruction of the silicon-oxygen network and for complete boron transformation significant excess of alkali oxides is required. In high-silica glasses (71-80 mol.% SiO_2) transformation is completed at $\psi_B \approx 1.8$ whereas at lower silica content the ψ_B value is much higher [6]. We have demonstrated using IR and electron paramagnetic resonance (EPR) spectroscopy that in borosilicate glasses for high-sodium intermediate level waste immobilization containing 40-50 wt.% SiO_2 minor fraction of trigonally coordinated boron is present even at $\psi_B \cong$ 4-5 [7].

Modifying oxides are different in their capability to be donors of oxygen and, in general, the ψ_B factor may be calculated as [6]

$$\psi_B = \{([Na_2O]+[K_2O]+[BaO])+0,7([CaO]+[SrO]+[CdO]+[PbO])+ 0.3([Li_2O]+[MgO]+[ZnO])-[Al_2O_3]\}/[B_2O_3] \quad (2)$$

where concentrations of oxides are given on a molar basis. At that, if glass does not contain ZnO and PbO, then all amount of Al_2O_3 is to be subtracted. If ZnO or/and PbO content exceeds Al_2O_3 content, then the correction is not done. Finally, if ZnO+PbO content is lower than that of Al_2O_3, then Al_2O_3 excess only is taken into account.

Because Al_2O_3 is a stronger acceptor of oxygen than B_2O_3, oxygen introduced with alkali and alkali earth oxides is initially used for transformation of Al into four-coordinated state. Scheme of coordination transformations for aluminoborosilicate glasses is shown in Table III [6].

Table III. Coordination of boron and aluminum in glasses at various ψ_B values [6].

φ_B	Coordination			
$\psi_B>1$	$[AlO_4]$	$[BO_4]$	-	-
$1/3<\psi_B<1$	$[AlO_4]$	$[BO_4]$	$[BO_3]$	-
$0<\psi_B<1/3$	$[AlO_4]$	-	$[BO_3]$	-
$\psi_B<0$	$[AlO_4]$	-	$[BO_3]$	$[AlO_6]$

As seen from Table III, aluminum has a negative effect on the transformation of trigonally coordinated boron into tetragonally coordinated boron. Stability of coordination state depends on a value of cationic to anionic radii ratio (r_c/r_a). For tetrahedral oxygen coordination this ratio ranges between 0.22 and 0.41 [8] (radius of O^{2-} anion is assumed to be 1.36 Å). Deviation from average value of the r_c/r_O^{2-} ratio expressed as $|\Delta| = [r_c/r_O^{2-}]_{av} - [r_c/r_O^{2-}]_{calc}$ may be considered as a measure of stability of tetrahedral coordination for the given cation. The values calculated from two different reference data are given in Table IV. Due to higher stability of $[AlO_4]$ tetrahedra as compared to $[BO_4]$ tetrahedra oxygen delivered by alkali oxides is initially used for formation of AlO_4 tetrahedra and at relatively high Al_2O_3 concentrations the majority of boron remains three-coordinated. Nevertheless, this does not have a negative effect on chemical durability of glasses, because the aluminosilicate glass network built from SiO_4 and AlO_4 tetrahedra with associated alkali ions is leach resistant [9,10].

Table IV. Cationic radii, cationic to oxygen anion radii ratios and their deviations from average value (0.315 Å) for tetrahedrally coordinated ions.

Cation	B^{3+}		Si^{4+}		Al^{3+}		Fe^{3+}	
Refs	[8]	[11]	[8]	[11]	[8]	[11]	[8]	[11]
r_c, Å	0.20	0.11	0.39	0.26	0.57	0.39	0.67	0.49
r_c/r_O^{2-}	0.15	0.08	0.29	0.19	0.42	0.29	0.49	0.36
$\|\Delta\|$	0.165	0.235	0.025	0.125	0.105	0.025	0.175	0.045

The effect of iron oxides on boron coordination in borosilicate glasses is more complicated. Fe^{3+} ions being network-formers act similarly to Al^{3+} ions forming FeO_4 tetrahedra and suppressing the $B^{III} \rightarrow B^{IV}$ transformation. However, since stability of $[Fe^{3+}O_4]$ tetrahedron is lower then that of $[AlO_4]$, the effect of Fe_2O_3 on $B^{III} \rightarrow B^{IV}$ transformation is weaker. Molar concentration of Fe_2O_3 should be subtracted like Al_2O_3 in eq. (2) but with a coefficient less than 1. Taking into account that the energy of Fe^{3+}—O bond is lower than that of the Al—O bond by ~3 times, this coefficient may be suggested to be ~3 as well. Therefore, in the numerator of the eq. (2) we have to subtract additionally ~0.3×[Fe_2O_3]. Thus, in the presence of Fe_2O_3, the ψ_B values for the glasses studied are somewhat lower (Table I). At high concentrations in glasses, Fe^{3+} ions may become network-modifiers with higher coordination number (CN=6) or form a separate crystalline phase – hematite (Fe_2O_3) or spinel, especially in the presence of Fe^{2+} ions or different transition metal ions (Mn^{2+}, Ni^{2+}, Co^{2+}, Cu^{2+}, Zn^{2+}) as well as Mg^{2+} and Al^{3+} ions. Fe^{2+} ions, if present, are network-modifiers, but often form spinel type phase.

RESULTS

As seen from Tables I and II, in both SB2 and SB4 waste glasses, Li_2O, B_2O_3 and SiO_2 concentrations in target and actual glasses and vitreous phases of the actual glassy materials gradually decrease whereas waste oxide concentrations, except Fe_2O_3, increase. Molar concentration of Fe_2O_3 in vitreous phases passes through a maximum at 55 wt.% WL in the SB2 glasses and at 50 wt.% WL in the SB4 waste glasses. The reason of this phenomenon is crystallization of magnetite or magnetite-trevorite type spinel accumulating significant fraction of Fe_2O_3.

Table II and Fig. 1 show that from a theoretical point of view neither the SB2 or SB4 waste glasses nor their vitreous phases can exist because the f_{Si} values are less than 0.33 at any waste loading. Nevertheless, vitrified products from these compositions contain a vitreous phase. This shows that not only SiO_2 (and B_2O_3) is a network-former but Al_2O_3 and at least some Fe_2O_3 exhibit network-forming properties as well.

The structure of the anionic motif of the glass network may be studied by various spectroscopic techniques, for instance, IR spectroscopy. Fig. 2 demonstrates changes in IR spectra of the glassy materials as a function of waste loading and thermal treatment.

Most of the glassy materials studied (except SB4 waste glasses at up to 50 wt.% WL) are composed of major vitreous and minor spinel structure phases. The latter has chemical composition corresponding to magnetite-trevorite [$(Fe,Ni)^{2+}$ $(Fe^{3+})_2O_4$] solid solution with trace

of Mn^{2+}, Mg^{2+}, Zn^{2+}, Cr^{3+}, Al^{3+} ions. IR spectra of all the vitrified wastes within the range of 1600-400 cm^{-1} consist of the bands at 1500-1300 cm^{-1} (moderate), 1200-800 cm^{-1} (strong), 800-650 cm^{-1} (weak), 600-400 cm^{-1} (strong) due to stretching and bending modes in silicon-oxygen, boron-oxygen, aluminum-oxygen and iron-oxygen structural groups.

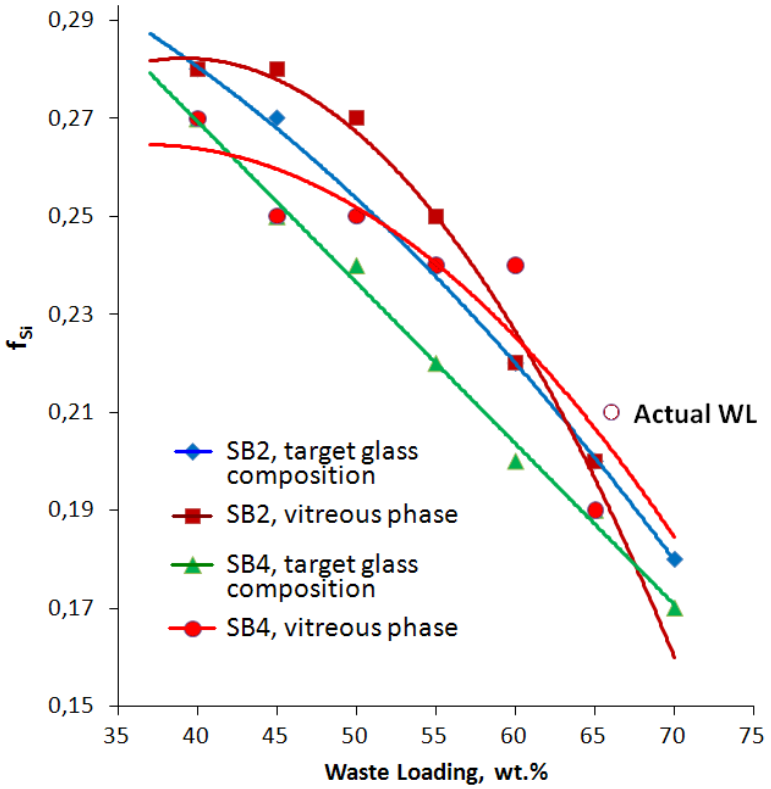

Fig. 1. Plot of f_{Si} vs WL for the vitrified SB2 and SB4 wastes and vitreous phases in them. Actual WL in the material with target 70 wt.% WL produced in a 236 mm inner diameter cold crucible was found to be ~66 wt.%.

Attribution of the band at 1500-1350 cm^{-1} normally observed in spectra of alkali-silicate glasses is confusing This band was associated with bending modes in metal hydroxides, structurally bound or absorbed water or stretching modes in CO_3^{2-} ions. In the spectra of borate and borosilicate glasses the wavenumber ranges of 1550-1300 cm^{-1} and ~1260-1270 cm^{-1} are typical of vibrations in the boron-oxygen groups with trigonally coordinated boron (boron-oxygen triangles BO_3). These bands were attributed as components of twice degenerated asymmetric valence ν_3 O−B−O vibrations (stretching modes). The band with components ~710-730 and 650-670 cm^{-1} may be associated with twice degenerated asymmetric deformation δ (ν_4) O−B−O vibrations (bending modes) [12]. Strong absorption in both IR and Raman spectra within the range of 1150-850 cm^{-1} is caused by asymmetric ν_3 vibrations (stretching modes) in silicon-oxygen units being isolated (850-900 cm^{-1}) or bound to one (~900-950 cm^{-1}), two (~950-1050 cm^{-1}), three (~1050-1100 cm^{-1}) and four (~1100-1150 cm^{-1}) neighboring SiO_4 tetrahedra (Q^0, Q^1, Q^2, Q^3, Q^4, respectively) [13] and, in less extent, BO_4 tetrahedra (1000-1100 cm^{-1}) [14]. In IR spectra of all the glasses, the broad band within the range of ~800-1200 cm^{-1} is multicomponent

due to superposition of vibrations (stretching modes) in SiO_4 and BO_4 tetrahedra. Stretching modes of Al—O bonds in AlO_4 tetrahedra and Fe—O bonds in FeO_4 tetrahedra are positioned at 700-800 cm^{-1} and 550-650 cm^{-1}, respectively. Bending modes of Si—O—Si bonds in SiO_4 tetrahedra are positioned within the range of 350-550 cm^{-1}.

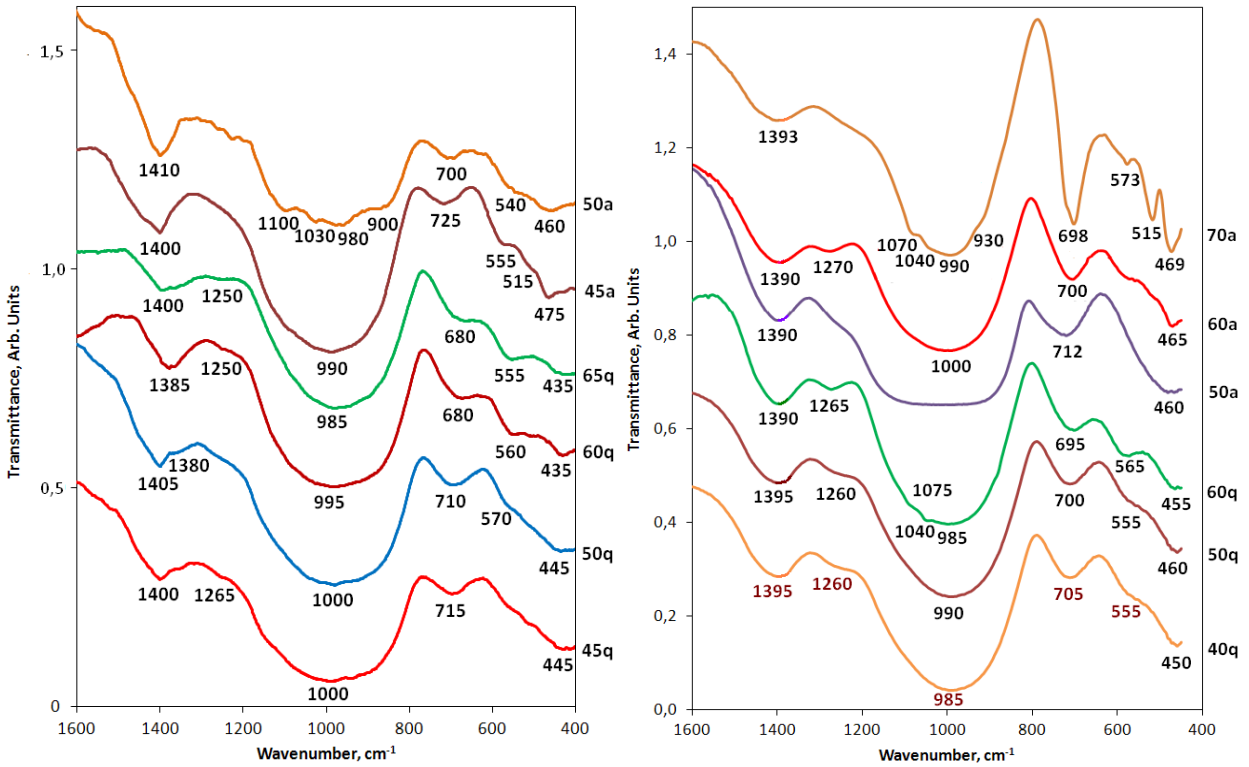

Fig. 2. IR spectra of SB2 (left) and SB4 (right) glasses at various waste loadings produced in a laboratory furnace and quenched onto a metal plate (q) and cold crucibles and slowly cooled (annealed) in canisters (a).

SB2 waste glass at 45 wt.% WL is composed of predominant vitreous phase and trace (<5 vol.%) of spinel structure magnetite phase [2,9,10]. IR spectrum of this glass (Figure 2, left) consists of the strong bands weak within the ranges of 1200-800 cm^{-1} and lower 600 cm^{-1}, weak bands at 1450-1350 cm^{-1} splitting into components at ~1400 cm^{-1} and ~1380 cm^{-1}, and 750-700 cm^{-1}, and a shoulder at ~1265 cm^{-1}. Weak bands at ~1380 cm^{-1} and ~715 cm^{-1}, shoulder at ~1265 cm^{-1} and high-wavenumber edge of the band lower 600 cm^{-1} may be attributed to vibrations in BO_3 groups. However, major contributions to absorption within the range of 750-700 cm^{-1} 600-500 cm^{-1} are due to vibrations in AlO_4 and FeO_4 tetrahedra because concentrations of their oxides in glass is higher.

The broad band within the range of 1200-800 cm^{-1} may be resolved into components centered at ~1000 cm^{-1} and ~920 cm^{-1} due to vibrations of Si—O bonds in SiO_4 Q^2 and Q^1-type tetrahedra. Some contribution to the low-wavenumber component probably give vibrations of Si—O—Fe bonds linking SiO_4 and FeO_4 tetrahedra [15].

With the increase of WL from 45 wt.% to 65 wt.% the band 1200-800 cm^{-1} becomes narrower and absorption in the low-wavenumber range builds up forming the band at ~555-560 cm^{-1} due to vibrations of Fe—O bonds in FeO_4 tetrahedra. Simultaneously, the maximum of the band 750-700 cm^{-1} is shifted from 715 cm^{-1} to ~680 cm^{-1} possibly due to partial formation of AlO_4 tetrahedra with one bridging oxygen ion or formation of nepheline.

Similar changes take place in the spectra of annealed materials produced in cold crucibles and sampled from canisters (Fig. 2). It is evident that there is a splitting of the bands within the ranges of 1300-800 cm^{-1} and below 600 cm^{-1} due to segregation of crystalline phases – spinel and nepheline.

IR spectra of the quenched glass containing 40 and 50 wt.% SB4 waste (Fig. 2, right) are somewhat similar to those of quenched SB2 waste glasses. Major features are a narrower band within the range 1200-800 cm^{-1} and a more defined shoulder at ~1260 cm^{-1} transformed into a clear band centered at 1265 cm^{-1}. This indicates higher fraction of trigonally coordinated boron in the SB4 waste glasses as compared to the SB2 waste glasses.

Similar to the spectra of annealed SB2 waste glasses, the spectra of annealed SB4 waste glasses show splitting of the bands at 1200-800 cm^{-1} and below 700 cm^{-1} (Fig. 2, right) due to partial devitrification of these glasses with crystallization of spinel and nepheline.

Fig. 3 demonstrates linear dependences between the ψ_B factor and WL for target glass compositions and significant scatter of experimental points for vitreous phase compositions for both SB2 and SB4 waste glasses. The errors are 8% and 13% of the indication for the ψ_B values calculated for the effect of Al_2O_3 only and combined Al_2O_3.

There is appreciable discrepancy between the ψ_B values for target glass compositions and compositions of vitreous phase which increases strongly with the increase of WL in glassy materials. The biggest discrepancy takes place between the ψ_B values for target SB2 waste glass composition and composition of its vitreous phase due to crystallization of magnetite-type spinel. In the SB4 waste glasses this effect is weaker. Crystallization of the nepheline phase in these glasses has an influence on the ψ_B value but not to a so strong extent because Na_2O and Al_2O_3 enter the nepheline phase in the same molar ratio as they are present in glasses (~1).

The ψ_B factor in the vitreous phase increases slowly with the increase of WL up to 50 wt.%. At WL of ~50 wt.% crystallization of spinel begins. Within the range of 50-60 wt.% WL, the biggest scatter of the ψ_B values is observed (Fig. 3). At ~60 wt.% WL and higher, crystallization of nepheline results in only a minor effect on the ψ_B value because the major factor influencing on strong increase of the ψ_B value is extraction of Fe_2O_3 from vitreous phase and reduction in B_2O_3 content. This effect is the most apparent in the SB2 waste glasses (Fig. 3).

The SB2 waste glasses for whose compositions the ψ_B values are more than 2 should have less tendency to liquid-liquid phase separation than the SB4 waste glasses ($\psi_B \leq$ ~1 for WL content $\leq$ 60 wt.%). Due to the low silica content, both homogeneous glasses at relatively low WLs (<55 w.%) and vitreous phases of the glass-crystalline materials at WLs of 55-65 wt.% should have appreciable fraction of trigonally-coordinated boron in their structures that is clearly confirmed by IR spectroscopic data (Fig. 2).

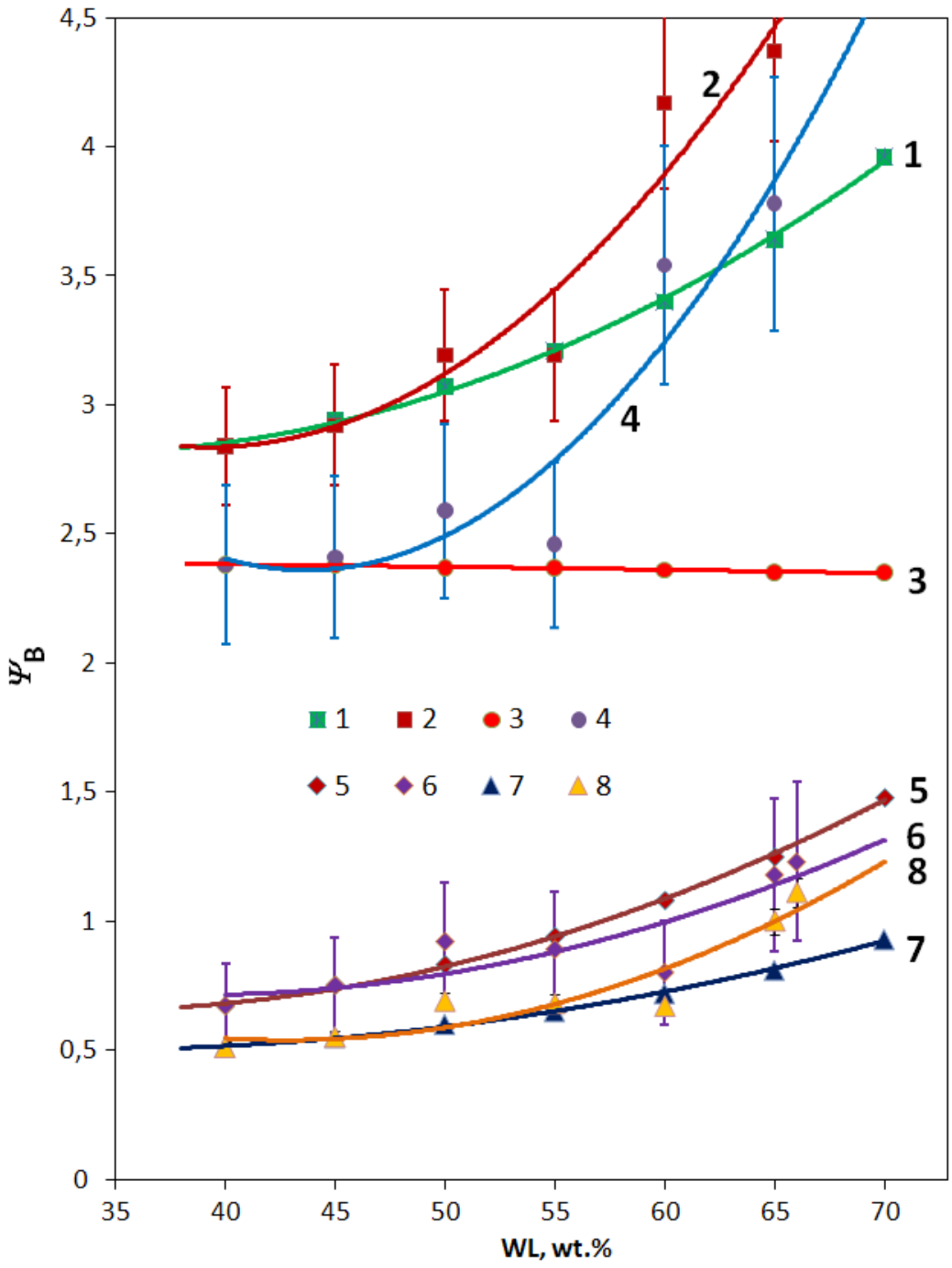

Fig. 3. Plot of ψ_B vs WL for SB2 (1-4) and SB4 (5-8) waste glasses with target compositions (1,3,5,7) and vitreous phases in the glassy materials (2,4,6,8) taking into account effect of Al_2O_3 only (1,2,5,6) and cumulative effect of Al_2O_3 and Fe_2O_3 (3,4,7,8) on ψ_B.

Summary of the values of normalized elemental mass release from SB2 and SB4 waste glasses is given in Table V. The effect of WL on normalized elemental molar release values from the SB2 and SB4 waste glasses is illustrated by Fig. 4.

Table V. Chemical durability of vitrified SB2 and SB4 wastes (PCT procedure).

Sample	Waste Loading, wt.%	Плавитель	Normalized Release, g/L			
			B	Li	Na	Si
SB2-35-JHCM	35 [16]	Ceramic melter, DWPF, SRNL	1.33	1.25	1.39	0.79
SB2-40-JHCM	40 [16]	Ceramic melter, DWPF, SRNL	1.47	1.31	1.60	0.79
SB2-45-B	45 [2]	236 mm Cold Crucible, RVF***	0.56	0.49	0.80	0.35
SB2-45-F	45 [2]	418 mm Cold Crucible, RVF	0.53	0.75	0.82	0.45
SB2-50-B	50 [2]	236 mm Cold Crucible, RVF	0.46	0.65	0.74	0.30
SB2-50-F	50 [2]	418 mm Cold Crucible, RVF	0.64	0.74	0.82	0.35
SB2-55-F	55 [2]	418 mm Cold Crucible, RVF	1.40	1.03	1.09	0.40
SB2-60-F	60	418 mm Cold Crucible, RVF	2.20	1.45	1.28	0.49
SB4-40-L	40 [17]	Pt/Rh crucible, quenching	0.50	0.63	0.35	0.33
SB4-40-L-CCC	40 [17]	Pt/Rh crucible, CCC*	0.45	0.63	0.35	0.34
SB4-40-B	40	236 mm Cold Crucible, RVF	0.28	0.48	0.36	0.26
SB4-45-L	45 [17]	Pt/Rh crucible, quenching	0.41	0.52	0.35	0.32
SB4-45-L-CCC	45 [17]	Pt/Rh crucible, CCC	0.41	0.52	0.35	0.32
SB4-50-L	50 [17]	Pt/Rh crucible, quenching	0.55	0.68	0.53	0.34
SB4-50-L-CCC	50 [17]	Pt/Rh crucible, CCC	0.33	0.48	0.34	0.28
SB4-50-B	50 [10]	236 mm Cold Crucible, RVF	0.48	0.60	0.65	0.28
SB4-50-F	50 [10]	418 mm Cold Crucible, RVF	1.00	0.90	0.60	0.34
SB4-55-L	55 [17]	Pt/Rh crucible, quenching	0.42	0.56	0.53	0.34
SB4-55-L-CCC	55 [17]	Pt/Rh crucible, CCC	0.59	0.75	0.49	0.32
SB4-55-B	55 [10]	236 mm Cold Crucible, RVF	0.81	0.72	0.57	0.27
SB4-60-B	60 [10]	236 mm Cold Crucible, RVF	0.66	0.71	0.57	0.32
SB4-63-B	63 [10]	236 mm Cold Crucible, RVF	0.77	0.89	0.65	0.25
SB4-65-B	65 [10]	236 mm Cold Crucible, RVF	0.95	0.88	0,69	0.23
SB4-66-B	70 (66**) [10]	236 mm Cold Crucible, RVF	4.32	3.30	0.90	0.20
Environmental Assessment (EA) Glass [18]			18.11	9.99	13.78	4.04

* Canister Centerline Cooling[i], ** Actual waste loading, *** Radon Vitrification Facility.

As seen from Table V all the normalized elemental releases (NER) for the glasses both produced under laboratory conditions, including cooled by a Canister Centerline Cooling (CCC) regime, and in the cold crucible remain lower than the values of the Environmental Assessment (EA) glass. The EA glass is the benchmark glass used for repository qualification in the U.S. Normally NERs (mass) are by 10 to 30 times lower than those for EA glass [18]. Even at very high WLs (up to 60 wt.% SB2 waste and up to 66 wt.% SB4 waste) the NERs from glass-crystalline materials containing spinel and nepheline are by ~5-20 times lower than those for the EA glass.

NER of B, Li, and Na increases with an increase in waste loading for glassy materials with both SB2 and SB4 wastes. With that said, at relatively low WLs (40-50 wt.%) NERs remain nearly constant (Fig. 4, *b*) or even reduced for the glasses annealed by the CCC regime (Fig. 4, *d*). Significant increase of NERs take place only at high WLs. The strongest increase takes place for B and Li whereas NL of Si changes were negligible. For all the glasses, Li was found to be the most leachable element due to small cationic radius. There is a symbiotic effect of NER of Li and B pointing to their occurrence in chemically different micro-regions in the glasses with

preferably lithium-borate composition. While structural factors of the glasses with the target compositions gradually changed, the dependences of structural factors from chemical composition for glasses formed vitreous phases of actual glass-crystalline materials produced in both Pt and cold crucibles may have extrema due to structural transformations and crystallization in glasses influencing NERs. The effect of the structure of glasses on their chemical durability requires further investigation.

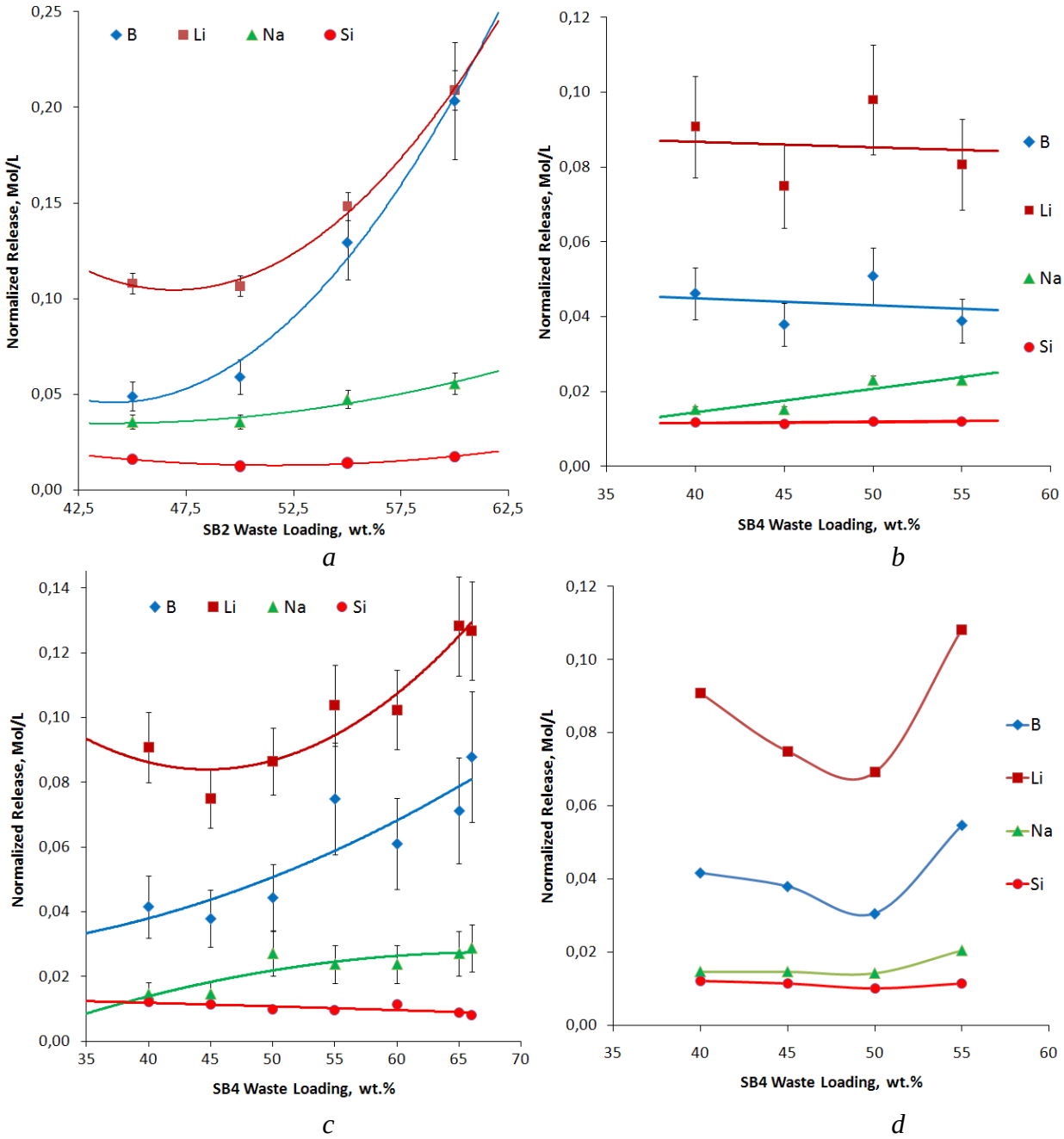

Fig. 4. Plot of normalized elemental release vs WL for SB2 waste glasses produced in cold crucibles (a) and SB4 waste glasses produced in lab-scale (50 cc) Pt crucibles, a 236 mm inner diameter cold crucible (c) and lab-scale Pt crucibles cooled by CCC regime (d)

CONCLUSIONS

Both the SB2 and SB4 waste glasses have very low formal values of the degree of connectedness (polymerization) of the silica-oxygen network. The actual degree of connectedness is higher due to incorporation of AlO_4 and FeO_4 tetrahedra in chains and rings of SiO_4 tetrahedra with formation of a common network. Boron is mostly trigonally coordinated by oxygen. In general, both SB4 waste glasses and vitreous phases of glasses containing crystals have much higher fraction of fourfold-coordinated boron in their structure than the materials containing SB2 waste because the SB4 glasses have high alumina contents. Aluminum ions have higher capacity to tie up oxygen ions to be converted to tetrahedral coordination than boron ions. Thus, AlO_4 (and some FeO_4) tetrahedra form complex units with alkali, primarily sodium ions, displacing trigonally coordinated boron and some fraction of alkali, primarily lithium ions. This results in separate micro-regions with different chemical composition and structure resulting in lower chemical durability than a homogeneous alkali aluminosilicate matrix. Formation of nepheline crystals in the matrix, at high waste loadings, may result in a decrease in chemical durability of glasses containing crystalline phases compared to homogeneous, amorphous glasses. Nevertheless, NERs from both SB2 and SB4 waste glasses were lower by 10 to 30 times lower than those for the EA glass.

REFERENCES

1. A.P. KOBELEV, S.V. STEFANOVSKY, O.A. KNYAZEV, T.N. LASHCHENOVA, A.G. PTASHKIN, M.A. POLKANOV, E.W. HOLTZSCHEITER, J.C. MARRA, “Results of a 50% Waste Loading Vitrification Test Using the Cold Crucible Melter for Savannah River Site,” Proc. Waste Management ’06 Conf. Tucson, AZ, February 26 – March 2, 2006. CD-ROM. ID 6127.
2. S.V. STEFANOVSKY and J.C. MARRA, “The Effect of Waste Loading on the Structure and Leach Resistance of Borosilicate Glass for Savannah River Site SB2 Waste Immobilization,” Proc. Waste Management ’07 Conf. Tucson, AZ, 2007. CD-ROM. ID 7132.
3. S.V. STEFANOVSKY, A.P. KOBELEV, V.V. LEBEDEV, M.A. POLKANOV, A.G. PTASHKIN, O.A. KNYAZEV, and J.C. MARRA, “Vitrification of Savannah River Site SB4 Waste Surrogate in the Radon Bench-Scale Cold Crucible Unit,” Proc. Int. Conf. Waste Management 2008, February 24 -28, 2008, Phoenix, AZ (2008) Paper # 8035.
4. S.V. STEFANOVSKY, A.P. KOBELEV, V.V. LEBEDEV, M.A. POLKANOV, A.G. PTASHKIN, O.A. KNYAZEV, and J.C. MARRA, “Cold Crucible Vitrification of SRS SB4 Waste at High Waste Loadings,” Proc. ICEM ’09 /DECOM ’09: 12th International Conference on Environmental Remediation and Radioactive Waste Management, October 11-15, 2009, Liverpool, UK (2009) Abstract, p. 122-123. CD-ROM. Paper #16197.
5. Standard Test Method for Determining Chemical Durability of Nuclear Waste Glasses: The Product Consistency Test (PCT). ASTM Standard C1285-94, ASTM, Philadelphia, PA (1994).
6. A.A. APPEN, “Chemistry of Glass,” (Russ., Nauka, Leningrad, 1974).
7. S.V. STEFANOVSKII, O.A. KNYAZEV, T.N. LASHCHENOVA, and S. MERLIN, *J. Adv. Mater.* **3** [6] (1996) 479-487.

8. G.B. BOKIY, “Crystal Chemistry,” (Russ., Moscow State University Publ., 1960).
9. S.V. STEFANOVSKY, A.P. KOBELEV, V.V. LEBEDEV, M.A. POLKANOV, D.Y. SUNTSOV, J.C. MARRA, “The Effect of Waste Loading on the Characteristics of Borosilicate SRS SB4 Waste Glasses,” ICEM ’09/DECOM ’09: 12th International Conference on Environmental Remediation and Radioactive Waste Management. October 11-15, 2009, Liverpool, UK. CD-ROM (2009).
10. A.P. KOBELEV, S.V. STEFANOVSKY, V.V. LEBEDEV, M.A. POLKANOV, V.V. GORBUNOV, A.G. PTASHKIN, O.A. KNYAZEV, J.C. MARRA, “Cold Crucible Vitrification of SRS SB4 HLW Surrogate at High Waste Loadings,” Advances in Materials Science for Environmental and Nuclear Technology. *Ceram. Trans*. **222** (2010) 91-104.
11. R.D. SHANNON, *Acta Cryst*. A32 (1976) 751-767.
12. V.A. KOLESOVA, *Glass Phys. Chem.* (Russ.) **12** [10] 4-13 (1986).
13. V.N. ANFILOGOV, V.N. BYKOV, A.A. OSIPOV, “Silicate Melts,” (Russ., Nauka, Moscow (2005).
14. I.I. PLUSNINA, “Infrared Spectra of Minerals,” (MGU, Moscow, 1977).
15. V. MAGNIEN, D.R. NEUVILLE, L. CORMIER, J. ROUX, J.-L. HAZEMANN, O. PINET, P. RICHET, *J. Nucl. Mater*. **352** (2006) 190-195.
16. C.C. HERMAN, “Summary of Results for Expanded Macrobatch 3 Variability Study,” WSRC-TR-2001-00511 (2001).
17. J.C. MARRA, K.M. FOX, D.K. PEELER, T.B. EDWARDS, A.L. YOUCHAK, J.H. GILLAM, JR., J.D. VIENNA, S.V. STEFANOVSKY, and A.S. ALOY, *Mat. Res. Soc. Symp. Proc.*,**1107** (2008) 231-238.
18. J.R. HARBOUR, “Summary of Results for Macrobatch 3 Variability Study,” WSRC-TR-2000-00351 (2000).